

Pressure-induced phonon softening and electronic topological transition in $\text{HgBa}_2\text{CuO}_4$

D. L. Novikov*

Science and Technology Center for Superconductivity, Department of Physics and Astronomy, Northwestern University, Evanston, Illinois 60208-3112

M. I. Katsnelson

Institute of Metal Physics, 620219 Ekaterinburg, Russia

Jaejun Yu

Department of Physics, Sogang University, Seoul, 121-742, Korea

A. V. Postnikov

Universität Osnabrück – Fachbereich Physik, D-49069 Osnabrück, Germany

A. J. Freeman

Science and Technology Center for Superconductivity, Department of Physics and Astronomy, Northwestern University, Evanston, Illinois 60208-3112

(Received 27 October 1995)

Total energy local density calculations for the effects of pressure on the lattice parameters, bond lengths, electronic structure, and A_{1g} phonon frequency in $\text{HgBa}_2\text{CuO}_4$ have been carried out in order to understand the role of pressure in increasing the T_c of mercury-based superconductors. Theoretically determined zero-pressure lattice parameters and phonon frequencies are found to be in good agreement with experiment. An electronic topological transition is found to occur when the van Hove singularity (vHS) is shifted close to the vicinity of E_F by pressure which causes considerable phonon softening and anomalous behavior of the c -axis length, the Hg-O(2) bond, and the Ba z coordinate. A set of experiments that might be able to detect the presence of the vHS close to E_F is proposed. [S0163-1829(96)01526-3]

I. INTRODUCTION

The discovery of the family of mercury compounds, $\text{HgBa}_2\text{Ca}_{n-1}\text{Cu}_n\text{O}_{2n+2+\delta}$ ($n=1,2,3, \dots, n$) [referred also as $\text{Hg-12}(n-1)n$],¹⁻⁷ has attracted a great deal of interest not only because of their record-breaking T_c 's but also due to their rich physical-chemical phenomena. The apparent simplicity of their crystal structure opens the way for very detailed experimental and theoretical investigations of high- T_c phenomena. The most exciting experimental work has been done on the effects of pressure on T_c (Refs. 8–14) and on the crystal structure of $\text{HgBa}_2\text{Ca}_{n-1}\text{Cu}_n\text{O}_{2n+2+\delta}$.¹⁵ The dependence of T_c on the unit cell volume of Hg-1223 in a small pressure region was determined in Ref. 16. These papers indicate that for low pressures T_c increases linearly as $dT_c/dP \approx +1.7-1.8$ K/GPa. And it was also found that at certain pressures T_c saturates or at least dT_c/dP decreases substantially.^{8,11} The value of dT_c/dP for Hg-based compounds is not unique in the whole family of high- T_c superconductors,¹⁵ but the high starting T_c value makes it possible to reach T_c 's as high as 164 K for Hg-1223 at high pressure.¹¹

The main question is whether it is possible to achieve such a T_c enhancement through chemical substitutions, i.e., by applying the chemical pressure. It is not yet clearly understood how such chemical pressure affects the phonon or electronic properties and thus the superconducting properties of high T_c Cu oxides. In fact, the role of phonons in the

mechanism of high- T_c superconductivity is not yet clearly established. There is experimental evidence in support of the phonon mechanism of superconductivity such as the strong isotope shifts observed in Y-Ba-Cu-O with a partial substitution of Pr for Y or La for Ba.^{17,18} On the other hand, there are other experiments that yield contradictions to the phonon-mediated picture of electron interactions (see, for instance, references in Ref. 19). Thus, the study of phonons seems to be very important in resolving the effects of electron-phonon interactions in high- T_c materials.

The phonon properties of the mercury family of superconductors have been the subject of very intensive study by Raman spectroscopy. It was found²⁰⁻²⁵ that the Raman spectra for all Hg-based superconductors display similar features: A strong peak at around 580 cm^{-1} was attributed to the apical oxygen vibrating along the c direction, the shoulder peak at a slightly lower frequency was speculated to be due to the presence of the interstitial oxygen, and weak features were observed around 180 cm^{-1} , which are thought to be due to Ba vibrations. The results of different experiments are put together in Table I.

A very interesting effort to understand the role of pressure in increasing T_c was undertaken in Ref. 24, where the effect of pressure on the Raman frequency ω of the apical oxygen for Hg-1201 and Hg-1212 was studied. The results show that ω of the apical oxygen [O(2)] A_{1g} mode increases with pressure and the rate of increase of the square of the normalized frequency, $\Delta(\omega/\omega_0)^2/\Delta P$, is nearly the same for Hg-1201

TABLE I. Comparison of experimental and theoretical frequencies of the Raman-active A_{1g} phonon mode. FLAPW, SM, and FLMTO refer to full-potential linearized augmented plane wave method, shell model, and full-potential LMTO method, respectively.

A_{1g} mode	Expt. ^a	Expt. ^b	Expt. ^c	FLAPW ^d	SM ^e	FLMTO ^e	FLMTO ^f
O(2)	592	592	591	587	591	540	586
Ba	161	158	—	—	124	161	158

^aReference 25.

^bReference 23.

^cReference 21.

^dReference 24.

^eReference 26.

^fThis work.

and Hg-1223 below ≈ 5 GPa, and is approximately 0.015 GPa^{-1} . For pressures above 5 GPa, $(\omega/\omega_0)^2$ for Hg-1201 keeps increasing linearly, while for Hg-1223 it changes its slope to 0.04 GPa^{-1} . The authors of Ref. 24 speculated that this difference in the $\omega(P)$ dependence may be attributed to a different response of the electronic structure to pressure in those materials. Another interesting feature of the Raman-active phonons in Hg-1201 is the softening of the phonon frequency of the apical oxygen A_{1g} mode below T_c .²⁵ It was also stated²⁵ that if this is a result of the appearance of the superconducting gap, the softening of such a high-frequency phonon would require the gap to be about $8.7k_B T$, which would be the highest known superconducting gap determined from Raman-active modes. Hence, regardless of one's view on the nature of high- T_c superconductivity (whether phonon mediated or not), the investigation of phonon properties provides important information for understanding the origin of high- T_c superconductivity. Moreover, the observed phonon softening implies the existence of a quite strong interaction of this particular phonon mode with the current carriers responsible for superconductivity. Thus, it is certainly important to investigate the influence of the electronic structure features on this particular phonon mode in Hg-based high- T_c superconductors.

The electronic structure of the Hg family has been studied intensively within the framework of the local density approximation (LDA).^{26–35} For the stoichiometric $\text{HgBa}_2\text{CuO}_4$ (Hg-1201) compound, it was found that the single band derived from the Cu-O antibonding state crossing the Fermi energy (E_F) is half-filled, and is thus expected to be a Mott insulator. With doping, however, it becomes a normal metal that becomes superconducting at 95 K. By contrast, there exists an additional Hg-O band crossing E_F in the case of $\text{HgBa}_2\text{CaCu}_2\text{O}_6$ (Hg-1212) and $\text{HgBa}_2\text{Ca}_2\text{CuO}_4\text{O}_8$ (Hg-1223), which makes them “self-doped” to a metallic normal state.^{27–35} In all cases, there exists a prominent van Hove singularity close to E_F , as was also found for other high- T_c cuprate materials [LSCO ($\text{La}_{2-x}\text{Sr}_x\text{CuO}_4$), (Ref. 36) YBCO ($\text{YBa}_2\text{Cu}_3\text{O}_7$) (Refs. 37–39), and the infinite layer compound ($\text{Sr}_x\text{Ca}_{x-1}\text{CuO}_2$) (Ref. 40)]. The apparent importance of the proximity of the vHS to the Fermi level leading to a large enhancement of the electron-phonon coupling coefficient λ for high- T_c materials was stressed by Andersen *et al.*³⁸ Recently a model was proposed,^{41–43} based on the “extended saddle point singularities” in the electron spectrum.

The effects of pressure on the electronic structure and lattice parameters for Hg-1201 ($\delta=0$) were studied by us²⁹ and for Hg-1212 ($\delta \neq 0$) by Singh.³⁰ We have shown that the energy location of the vHS moves towards E_F with increasing pressure and that there is a correspondence between hole doping and pressure treatments.²⁹ A calculation of the phonon dispersion relation and phonon density of states in the framework of the shell model for Hg-1201, together with an *ab initio* full-potential linear muffin-tin orbital (FLMTO) determination of frequencies and eigenvectors of the Raman-active modes (using experimental lattice parameters), was reported by Stachiotti *et al.*²⁶ They found a reasonable agreement between two A_{1g} and two E_g Raman-active zone center modes and experiment (see Table I).

Signifying the important role of phonons in high- T_c , there has been an experimental study²⁴ on the phonon properties under pressure in Hg-based high- T_c superconductors. Thus, in order to advance the understanding of the phonon properties of the high- T_c superconductors, we have undertaken an *ab initio* LDA simulation of the effect of pressure on the phonon spectra of Hg-1201. For the sake of simplicity we used $\delta=0$. The actual doping can vary between 0.04 and 0.23.⁴⁴ It was also found⁴⁴ that $\delta=0.18$ corresponds to the highest (or optimum) T_c value, which turns out to be surprisingly close to our prediction²⁸ if one assumes that oxygen acts as a divalent ion in doping Hg layers. We believe our simulation of Hg-1201 with $\delta=0$ should well describe the real system, if δ is “not too high.”

In this paper, we extend our previous investigation²⁹ of the effects of pressure on Hg-1201 and report results of LDA simulations of pressure effects on the electronic structure, lattice parameters, and A_{1g} phonon mode frequency. We find that the pressure-induced shift of the vHS towards E_F drives a softening of the A_{1g} phonon frequency. We also discuss some possible consequences of the electronic topological transition (ETT) due to the presence of the vHS crossing E_F , as predicted by Lifshitz.⁴⁵ Possible thermopower, bulk moduli, and thermal expansion coefficient experiments are discussed in relation to the effects of the ETT driven by the vHS.

II. METHOD AND COMPUTATIONAL DETAILS

We used the full-potential linear muffin-tin orbital method (FLMTO) (Refs. 46–49) within LDA and the Ceperly-Alder form of the exchange correlation potential.⁵⁰ The details of

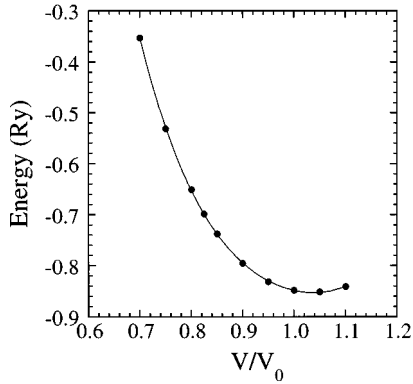


FIG. 1. Total energy as a function of volume for optimized c/a , $z_{O(2)}$, and z_{Ba} (solid circles) and a polynomial fit to these points.

our setup are similar to those used in our previous simulations.²⁹

Using calculated FLMT0 total energy results, we optimized the geometry of the unit cell of Hg-1201 for different unit cell volumes ($V/V_0 = 1.1, 1.05, 1.0, 0.95, 0.9, 0.85, 0.8, 0.75, 0.7$), where V_0 is the experimental volume. Note that we have extended the range of volume variation from that used earlier.²⁹ The optimization for each particular volume was carried out in the three-dimensional space of the parameters c/a , $z_{O(2)}$ (the z coordinate of the apical oxygen) and z_{Ba} (the Ba z coordinate). A symmetry analysis of the phonon modes and an estimation of frequencies were performed using a program developed by one of us.^{51,52}

III. RESULTS OF THE LDA SIMULATION

A. Effects of pressure on lattice parameters

The calculated FLMT0 total energy results were used to find the equation of state [$V(E)$] for Hg-1201. The calculated points (for different V/V_0) and their fourth-order polynomial fit are presented in Fig. 1. The equation of state allows us to find an analytic dependence of the unit cell volume on pressure [$P = -\partial E(V)/\partial V$] (cf. Fig. 2). The pressure dependence of the c and a lattice parameters along with the Hg-O(2) and Cu-O(2) bond lengths and the z_{Ba} coordinate are presented in Fig. 3. For comparison, the calculated

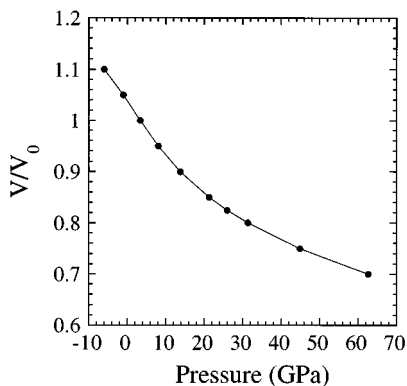


FIG. 2. Calculated volume as a function of pressure for Hg-1201.

lattice parameters and selected bond lengths together with experimentally determined values¹⁵ and estimated differences between them are presented in Table II. As seen, our theoretical values differ from experiment¹⁵ in the range between 0.6% and 3%. The largest discrepancy of -3% comes from an underestimation of the c/a ratio; the a parameter is overestimated by 2%. Although such a discrepancy is already small for the LDA approach, we note that we compare the results of calculations for $\delta=0$, while reliable experimental values are available only for doped materials.¹⁵ The agreement seems to be quite good especially if one takes into account that the a lattice parameter tends to decrease with doping, as was recently shown by Huang *et al.*,⁴⁴ and that the c parameter displays more complicated behavior.⁴⁴ It increases with doping in the region close to $\delta=0$ and reaches its maximum at a certain doping. Thus, if we extrapolate the experimental values to $\delta=0$, our results for zero pressure seem to be in even better agreement with experiment.

As seen from Fig. 3, the c axis is more compressible than the a axis (see also Ref. 29). As shown previously,²⁹ the main contribution to this anisotropy comes from the highly compressible Cu-O(2) bond. The calculated bond and axis compressibilities are in satisfactory agreement with experiment¹⁵ and with model calculations,⁵³ especially if one takes into account the sensitivity of the lattice parameters to doping⁴⁴ discussed above. The fact that the Cu-O(2) bond is extremely compressible has a strong effect on the energy bands at the Fermi energy (E_F):²⁹ The shape of the Cu-O(1) $d\rho\sigma$ half-filled band changes under pressure in such a way that the van Hove singularity (vHS), also called a singular point with an energy E_c that exists at ≈ 0.4 eV below E_F (at zero pressure) moves up with pressure and eventually crosses it (see Figs. 5 and 6 in Ref. 29). If correct, this fact leads to a good possibility to examine the effects of the vHS approaching E_F on the physical properties of the high- T_c superconductors, since the direct simulation of doping, which also changes E_F and apparently leads to an optimum T_c when it coincides with the vHS (see, for example, the review by Markiewicz⁵⁴), is usually not possible. Obviously, experimental evidence of vHS manifestations can greatly improve the understanding of high- T_c phenomena.

Another interesting feature is a nonmonotonic pressure dependence of the c -axis lattice parameter, Cu-O(2) bond lengths, and Ba position in Hg-1201 as shown in Fig. 3. In Fig. 3(b), it is emphasized that the calculated values (solid circles) are fitted in two different pressure regions (called I and II on our figures) by different linear interpolations: the region (I) from -10 GPa to ≈ 25 GPa (the negative pressure corresponds to unit cell stretching) and the region (II) above 25 GPa. In fact, the c parameter simply follows the Cu-O(2) bond behavior since the Hg-O(2) bond changes linearly with pressure and by only a very small amount (cf. Fig. 3). It is interesting to note that the kink in the pressure dependence of the Cu-O(2) bond length occurs at the pressure at which the vHS crosses E_F . Therefore, similar anomalies in the phonon modes are expected to occur at pressures where the vHS approaches E_F .

B. Effects of pressure on the A_{1g} phonon frequency

Since the only available experimental data on the pressure dependence of the phonon modes in Hg-1201 are for the

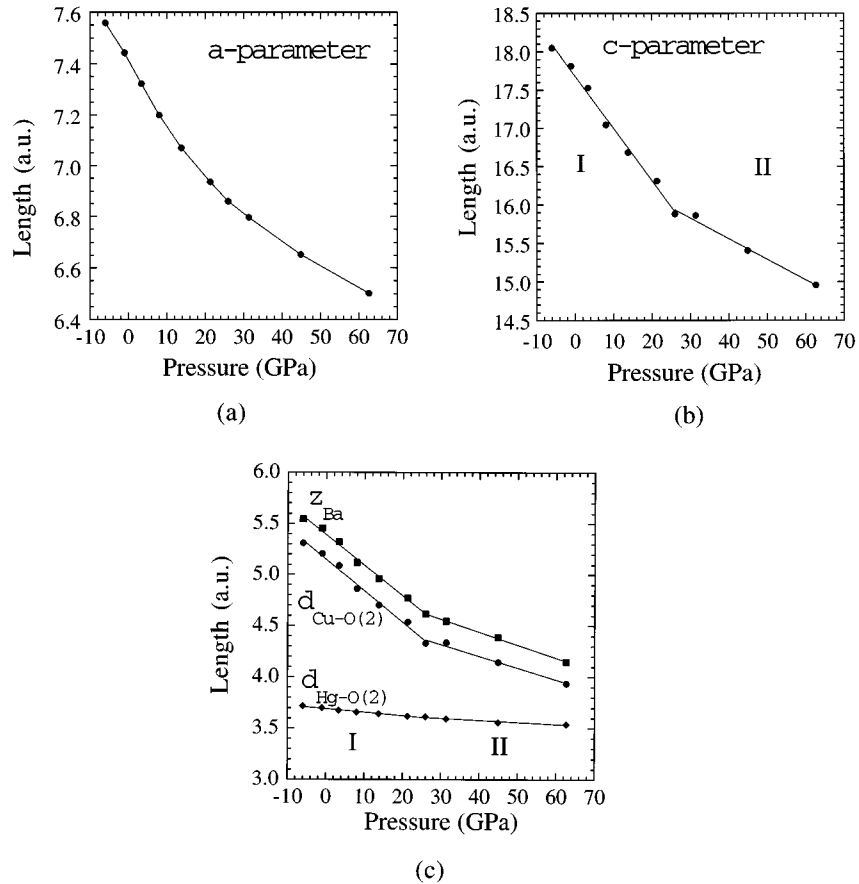


FIG. 3. Lattice parameters as functions of pressure for two distinct pressure regions (I and II): (a) a parameter; (b) c parameter, (c) Hg-O(2) and Cu-O(2) bond lengths and Ba z coordinate.

A_{1g} Raman-active mode,²⁴ we concentrate our attention on it. As follows from a symmetry analysis, the A_{1g} phonon represents O(2) and Ba vibrations along the z direction. We have calculated the total energy (frozen phonon approximation) for a sufficient number of independent O(2) and Ba displacements (usually the mesh is 14×14) to make a fit by a sixth-order polynomial. Such a high-order polynomial was needed to describe satisfactorily the strongly anharmonic total energy surface. A slice of the total energy surface along the O(2)-displacement coordinate axis (Fig. 4) clearly shows the anharmonicity of the O(2) vibrations.

The calculated O(2) and Ba A_{1g} phonon frequencies for different pressure, $\omega_{O(2)}(P)$ and $\omega_{Ba}(P)$, are plotted in Fig. 5. Frequencies for both atoms start increasing linearly with pressure. Both display a striking feature — a dip that occurs

around the pressure at which the vHS passes through E_F . After that, they proceed linearly with further increase of pressure. Since both $\omega_{O(2)}(P)$ and $\omega_{Ba}(P)$ show two distinct linear regions (I and II), we fit the calculated points with different linear functions in those regions. The fitting coefficients are listed in the inset in Fig. 5. From this fit we estimate the frequencies corresponding to zero pressure to be $\omega_{O(2)} = 586 \text{ cm}^{-1}$ and $\omega_{Ba} = 158 \text{ cm}^{-1}$ and their rate of increase with pressure as $d\omega_{O(2)}/dP = 3.9 \text{ cm}^{-1}/\text{GPa}$ and $d\omega_{Ba}/dP = 1.2 \text{ cm}^{-1}/\text{GPa}$ for pressure region I and $1.68 \text{ cm}^{-1}/\text{GPa}$ and $0.23 \text{ cm}^{-1}/\text{GPa}$ for pressure region II. These zero-pressure frequencies appear to be in excellent agree-

TABLE II. Experimental (Ref. 15) and calculated lattice parameters and selected bond length (in a.u.) for Hg-1201 and their percentage deviations (+ and - indicate overestimation and underestimation).

	Experiment	Theory	Deviation
a	7.332	7.500	+2%
c/a	2.455	3.691	-3%
Hg-O(2)	3.734	2.390	-1%
Cu-O(2)	5.257	5.150	-2%
Z_{Ba}	5.360	5.391	+0.6%

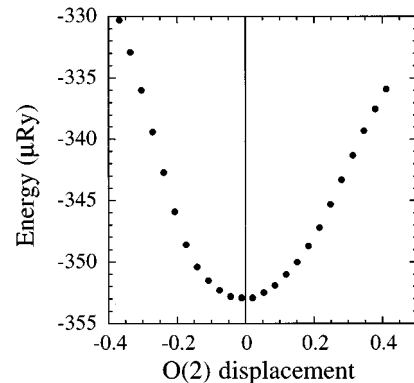


FIG. 4. Total energy vs O(2) displacements.

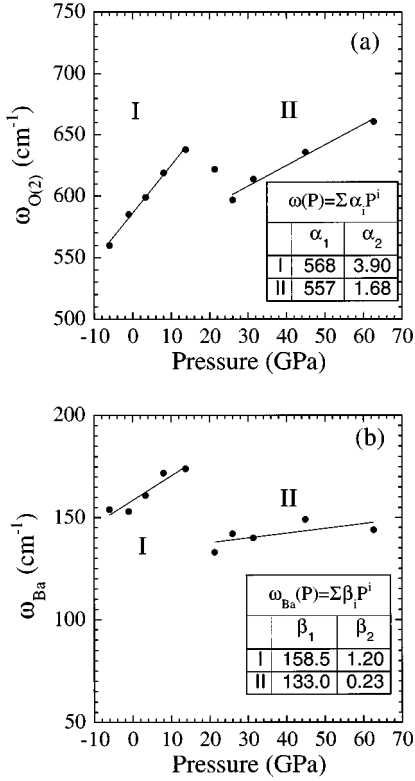


FIG. 5. The calculated (a) O(2) and (b) Ba A_{1g} phonon frequency [$\omega_{O(2)}(P)$ and $\omega_{Ba}(P)$] for different pressures and coefficients of a linear least-squares fit to them in different pressure regions (I and II).

ment with experiment and in good agreement with those calculated previously²⁶ at the experimental lattice parameters (cf. Table I).

In order to further compare our results on the pressure dependence of the phonon modes with experiment,²⁴ we have calculated the square of the normalized frequencies $(\omega/\omega_0)^2$. The calculated points and a least-squares linear fit to them (again in two distinct pressure regions I and II) are presented in Fig. 6. The values of $\Delta(\omega^2/\omega_0^2)/\Delta(P)$ can be also found in Fig. 6. For O(2), the A_{1g} mode $\Delta(\omega^2/\omega_0^2)_{O(2)}/\Delta(P)$ is about 0.014 GPa^{-1} which is in strikingly good agreement with the experimental value of 0.015 GPa^{-1} (Ref. 24) for Hg-1201 over the pressure range from 0 to 10 GPa. The corresponding value in the ‘‘high-pressure region’’ (II) is 0.006 GPa^{-1} . For $\Delta(\omega^2/\omega_0^2)_{Ba}/\Delta(P)$ we have 0.016 GPa^{-1} and 0.003 GPa^{-1} for the I and II pressure regions, respectively. Since we reproduce the experimental trend for the low-pressure part of $\omega(P)$, we may be quite confident in our results for higher pressures, including the softening of the A_{1g} mode in the pressure region where the vHS comes close to and passes through E_F .

Despite our initial hope to interpret the results of phonon frequency measurements for Hg-1223 (Ref. 24) on the basis of our calculations for Hg-1201, we cannot clearly see the reason for the kink in $(\omega/\omega_0)^2$ at pressures around 5 GPa for Hg-1212. It was previously supposed²⁴ that this kink originates from the fact that Hg-O(2)-derived band [which is located above E_F in Hg-1201 and slightly below E_F in Hg-1212 and Hg-1223 (Ref. 28)] moves down with pressure,²⁹

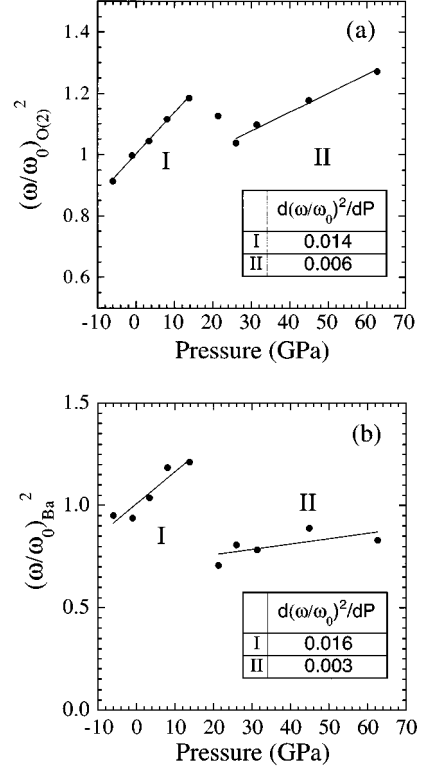


FIG. 6. Square of the normalized frequencies $(\omega/\omega_0)^2$ for different pressures and coefficients of a linear least-squares fit to them in different pressure regions (I and II).

becomes populated, and changes the strength of Hg-O(2) bond, which in turn affects the frequency of O(2) vibrations. But our calculations do not support this idea. Moreover, since this Hg-O(2)-derived band is *antibonding*, one might expect a *softening* of the Hg-O(2) bond and thus a decrease in the O(2) phonon frequency. Further, the effect of filling the Hg-O(2)-derived band on the calculated O(2) phonon frequency was not observed in our simulations. Hence, we have to conclude that the change in this band population is too small to produce an observable effect and so this particular result of the phonon frequency measurements²⁴ still remains unresolved.

IV. POSSIBLE PHYSICAL CONSEQUENCES OF THE vHS EXISTING CLOSE TO E_F

As was mentioned in the Introduction, vHS-based models of high- T_c superconductivity have recently attracted considerable attention.¹⁹ The models try to establish the connection between anomalies in the physical properties of the high- T_c materials and the existence of a vHS close to E_F . As we have shown previously for the infinite layer compound⁴⁰ and for Hg-1201 and Hg-1212,^{28,27} there is an apparent correlation between T_c as a function of doping and/or pressure and a maximum in the density of states, located close to E_F . Or, in other words, the behavior of T_c depends strongly on the vHS passing close to or through E_F ; the latter case is known as an electronic topological transition (ETT).⁴⁵ The direct proof of this hypothesis would be experimental observations of those properties of high- T_c materials that are sensitive to this ETT. These include thermopower,⁵⁵ bulk modulus,^{56–59} phonon frequencies, and thermal expansion coefficients.

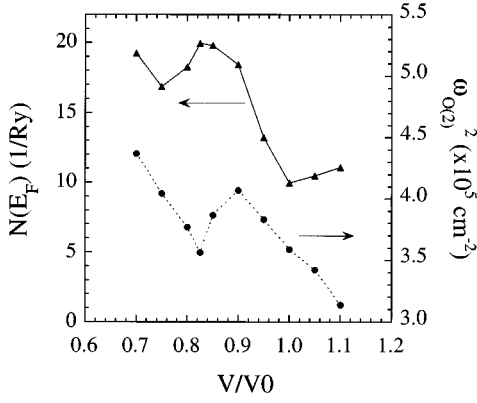


FIG. 7. $\omega_{(2)}^2$ and $N(E_F)$ for different unit cell volumes of Hg-1201.

The thermopower α (in the nonsuperconducting state) must display very sharp anomalies of the type $\delta\alpha \sim T \partial N(E_F) / \partial E_F$ (Ref. 55) as a function of pressure or doping. Unfortunately, these anomalies can be seen clearly only at very low temperatures (see, e.g., Refs. 60,61) and so they might be difficult to measure in superconductors with high critical temperatures. One possible way to detect an ETT in such systems is to conduct low-temperature measurements with the superconductivity suppressed by a high magnetic field. However, it might be more convenient to detect anomalies in the lattice properties at a not too low temperature. Corresponding expressions for the ETT in the two-dimensional case [i.e., the logarithmic anomaly in $N(E_F)$ caused by a saddle point] were derived in an almost-free-electron approximation in Ref. 62 in connection with a discussion of magnetovolume and magnetoelastic effects in itinerant ferromagnets.

To be specific, let us consider the anomalies in the elastic moduli,

$$C_{ii} = \frac{1}{\Omega} \frac{\partial^2 E}{\partial u_i^2}, \quad (1)$$

where Ω is a unit cell volume, E is the total energy, and u_i the corresponding deformation (acoustical or optical). In the case of optical deformations, when $\Omega C_{ii} = M \omega_i^2$ (where M is the atomic mass) and ω_i^2 is the corresponding Γ phonon frequency, we have⁵⁸

$$\Omega \delta C_{ii} = -\frac{1}{\sqrt{2}} \delta N(E_F) \left[\frac{\partial(E_F - E_c)}{\partial u_i} \right]^2. \quad (2)$$

Here $\delta N(E_F)$ is a vHS contribution to the density of states (DOS) at the Fermi level. [We stress that Eq. (2) describing the δC_{ii} anomaly is rather general and only the $1/\sqrt{2}$ pre-factor is model dependent.⁵⁸] It follows from Eq. (2) that a change of the squared frequency is proportional to the total DOS variation (due to the presence of vHS) with inverted sign. Or, simply, the squared frequency displays a minimum at the point of the maximum in the total DOS. We illustrate this in Fig. 7, where our numerical results for $\omega_{(2)}^2$ and $N(E_F)$ are plotted for different unit cell volumes.

Anomalies in the squared phonon frequency averaged over the Brillouin zone, ω^2 , due to an ETT are considerably

weaker than those for C_{ii} and are of the order of $(E_F - E_c) \delta N(E_F)$.^{57,58,62} For the almost-free-electron model,⁶² we have for the anomalous contribution to the averaged frequency squared

$$\overline{\delta M \omega^2} = \frac{2}{3} \mathbf{g}^2 |V_g| (E_F - E_c) \delta N(E_F), \quad (3)$$

where $\delta N(E_F)$ is the contribution of the vHS to the $N(E_F)$, M is the atomic mass (the lattice without basis was considered in Ref. 62), \mathbf{g} is the reciprocal lattice vector (the vHS is located at $k_c = g/2$), and V_g is the corresponding Fourier component of the crystal potential.⁶² For

$$T \geq T_c \approx \Theta_D \frac{(|V_g| |E_F - E_c|)^{1/2}}{E_F}, \quad (4)$$

where Θ_D is the Debye temperature, the anomaly in the thermal expansion coefficient^{57,62}

$$\beta(T) = \frac{1}{\Omega} \left(\frac{\partial \Omega}{\partial T} \right)_P = \frac{C_v}{B} \gamma \quad (5)$$

can be written down as

$$\begin{aligned} \delta \gamma &= -\frac{1}{2} \delta \frac{\partial \ln \omega^2}{\partial \ln \Omega} = \frac{B}{2M\omega^2} \frac{\partial}{\partial P} (\overline{M\omega^2}) \\ &= \frac{B g^2}{3M\omega^2} |V_g| \frac{\partial(E_F - E_c)}{\partial P} \delta N(E_F). \end{aligned} \quad (6)$$

Here $B = -\partial P / \partial \Omega$ is the bulk modulus, $C_v(T)$ is the lattice heat capacity, and γ is the Grüneisen parameter. The effect can be estimated as

$$\frac{\delta \beta}{\beta} \sim \frac{2|V_g|}{\Omega_0} \frac{\partial(E_F - E_c)}{\partial P} \delta N(E_F), \quad (7)$$

where $2|V_g|$ is the band splitting at the Brillouin zone boundary. In our case $\partial(E_c - E_F) / \partial P > 0$, and so $\delta \beta < 0$. Thus, if the maximum in T_c corresponds to the ETT, the thermal expansion coefficient β must have a minimum (or perhaps even become negative) near the ETT. At low temperatures, the sign of the anomalous contribution to β is the same, but the anomaly gets stronger [i.e., $1/(E_c - E_F)$ instead of $\ln|E_c - E_F|$].⁶²

Thus, we propose the following ‘‘tests’’ to detect the ETT in high- T_c materials when subjected to either pressure or doping. One should look (1) for a minimum in the phonon frequencies of the A_{1g} mode; it appears that the position of the vHS is especially sensitive to the deformation along the c axis, as we have shown in Sec. III, and thus anomalies in this phonon mode should be especially strong; (2) for a minimum in the thermal expansion coefficient; or (3) for strong anomalies in the thermopower at low temperatures when superconductivity is suppressed by high magnetic fields.

We have to mention also that it is quite possible that the first type of anomaly has already been observed, although indirectly. It was reported⁴⁴ that the maximum in T_c correlates with the maximum in the ratio of mean square amplitudes of Ba displacement along the c axis and in the ab

plane. At first glance, this looks puzzling since Ba states do not contribute to the DOS at E_F and apparently have nothing to do with superconductivity. By symmetry, however, Ba vibrations are connected to O(2) vibrations and their softening by the ETT causes the amplitude enhancement of the thermal vibrations in the c direction. At the same time, Ba vibrations in the ab plane are practically insensitive to the position of the vHS, as will be discussed in detail in a future paper.

ACKNOWLEDGMENTS

This work was supported by the National Science Foundation (through the Northwestern University Science and Technology Center for Superconductivity, Grant No. DMR 91-20000, and by a grant of computer time at the Pittsburgh Supercomputing Center supported by its Division of Advanced Scientific Computing). J.Y. acknowledges the support by the Korea Science Engineering Foundation (Grant No. 951-0209-010-2).

- *On leave from Institute of Solid State Chemistry, Russian Academy of Sciences, Ekaterinburg, Russia. Electronic address: d-novikov@nwu.edu
- ¹S. N. Putilin, E. V. Antipov, O. Chmaissem, and M. Marezio, *Nature (London)* **362**, 226 (1993).
 - ²S. N. Putilin, E. V. Antipov, and M. Marezio, *Physica C* **212**, 266 (1993).
 - ³A. Schilling, M. Catoni, J. D. Guo, and H. R. Ott, *Nature (London)* **363**, 56 (1993).
 - ⁴L. Gao *et al.*, *Physica C* **251**, 261 (1993).
 - ⁵M. Catoni, A. Schilling, H.-U. Nissen, and H. K. Ott, *Physica C* **215**, 11 (1993).
 - ⁶R. L. Meng *et al.*, *Physica C* **216**, 21 (1993).
 - ⁷J. L. Wagner *et al.*, *Physica C* **210**, 447 (1993).
 - ⁸C. W. Chu *et al.*, *Nature (London)* **365**, 97 (1993).
 - ⁹M. Nuñez-Regueiro *et al.*, *Science* **262**, 97 (1993).
 - ¹⁰A.-K. Klehe, A. K. Gangopadhyay, J. Diederichs, and J. S. Schilling, *Physica C* **213**, 266 (1992).
 - ¹¹L. Gao *et al.*, *Phys. Rev. B* **50**, 4260 (1994).
 - ¹²A.-K. Klehe, J. S. Schilling, J. L. Wagner, and D. G. Hinks, *Physica C* **223**, 313 (1994).
 - ¹³M. Kosuge, A. Tokiwa-Yamamoto, H. Yamauchi, and N. Koshizuka, *Physica C* **225**, 218 (1994).
 - ¹⁴Y. S. Yao *et al.*, *Physica C* **224**, 91 (1994).
 - ¹⁵B. A. Hunter *et al.*, *Physica C* **221**, 1 (1994).
 - ¹⁶C. C. Kim *et al.*, *Phys. Rev. B* **50**, 13778 (1994).
 - ¹⁷J. P. Franck *et al.*, *Physica B* **169**, 697 (1991).
 - ¹⁸H. J. Bornemann and D. E. Morris, *Phys. Rev. B* **44**, 5322 (1991).
 - ¹⁹A. A. Abrikosov, *Physica C* **244**, 243 (1995).
 - ²⁰Y. T. Ren *et al.*, *Physica C* **217**, 273 (1993).
 - ²¹Y. T. Ren *et al.*, *Physica C* **226**, 209 (1994).
 - ²²I.-S. Yang *et al.*, *Physica C* **218**, 365 (1993).
 - ²³N. H. Hur *et al.*, *Physica C* **218**, 365 (1993).
 - ²⁴I.-S. Yang *et al.*, *Phys. Rev. B* **51**, 644 (1995).
 - ²⁵M. C. Krantz, C. Tompsen, H. Mattausch, and M. Cardona, *Phys. Rev. B* **50**, 1165 (1995).
 - ²⁶M. G. Stachiotti *et al.*, *Physica C* **243**, 207 (1995).
 - ²⁷D. L. Novikov and A. J. Freeman, *Physica C* **212**, 233 (1993).
 - ²⁸D. L. Novikov and A. J. Freeman, *Physica C* **216**, 273 (1993).
 - ²⁹D. L. Novikov and A. J. Freeman, *Physica C* **222**, 38 (1994).
 - ³⁰D. J. Singh, *Physica C* **212**, 228 (1993).
 - ³¹D. J. Singh and W. Pickett, *Phys. Rev. Lett.* **73**, 476 (1994).
 - ³²C. O. Rodriguez, *Phys. Rev. B* **49**, 1200 (1994).
 - ³³C. O. Rodriguez, N. E. Christensen, and E. L. Peltzer y Blanká, *Physica C* **216**, 12 (1993).
 - ³⁴C. O. Rodriguez *et al.*, *Physica C* **219**, 17 (1994).
 - ³⁵C. O. Rodriguez, R. Weht, M. Weissmann, and N. E. Christensen, *Physica C* **235-240**, 2111 (1994).
 - ³⁶J. H. Xu, T. Watson-Yang, J. Yu, and A. J. Freeman, *Phys. Lett. A* **120**, 489 (1987).
 - ³⁷W. E. Pickett, R. E. Cohen, and H. Krakauer, *Phys. Rev. B* **42**, 8764 (1990).
 - ³⁸O. K. Andersen *et al.*, *Physica C* **185-189**, 147 (1991).
 - ³⁹S. Massida, J. Yu, and A. J. Freeman, *J. Phys. Chem. Solids* **52**, 1503 (1991).
 - ⁴⁰D. L. Novikov, V. A. Gubanov, and A. J. Freeman, *Physica C* **210**, 301 (1993).
 - ⁴¹A. A. Abrikosov, J. C. Campuzano, and K. Gofron, *Physica C* **214**, 73 (1993).
 - ⁴²A. A. Abrikosov, *Physica C* **222**, 191 (1994).
 - ⁴³A. A. Abrikosov, *Physica C* **233**, 102 (1994).
 - ⁴⁴Q. Huang, J. W. Lynn, Q. Xiong, and C. W. Chu, *Phys. Rev. B* **52**, 462 (1995).
 - ⁴⁵I. M. Lifshitz, *Sov. Phys. JETP* **11**, 1130 (1960).
 - ⁴⁶M. Methfessel, *Phys. Rev. B* **38**, 1537 (1988).
 - ⁴⁷M. Methfessel, C. O. Rodriguez, and O. K. Andersen, *Phys. Rev. B* **40**, 2009 (1989).
 - ⁴⁸A. T. Paxton, M. Methfessel, and H. Polatoglu, *Phys. Rev. B* **42**, 8127 (1990).
 - ⁴⁹M. Methfessel and M. Scheffler, *Phys. Rev. B* **172**, 175 (1991).
 - ⁵⁰D. M. Ceperley and B. J. Alder, *Phys. Rev. Lett.* **45**, 566 (1980).
 - ⁵¹A. V. Postnikov, T. Neumann, and G. Borstel, *Phys. Rev. B* **50**, 758 (1994).
 - ⁵²A. V. Postnikov and G. Borstel, *Phys. Rev. B* **50**, 16403 (1994).
 - ⁵³A. L. Cornelius and J. S. Schilling, *Physica C* **218**, 369 (1993).
 - ⁵⁴R. S. Markiewicz, *Physica C* **217**, 381 (1993).
 - ⁵⁵V. G. Vaks, A. V. Trefilov, and S. V. Fomichev, *Sov. Phys. JETP* **53**, 830 (1981).
 - ⁵⁶V. G. Vaks and A. V. Trefilov, *J. Phys. F* **18**, 213 (1988).
 - ⁵⁷V. G. Vaks and A. V. Trefilov, *J. Phys. Condens. Matter* **3**, 1389 (1991).
 - ⁵⁸M. I. Katsnelson, I. I. Naumov, and A. V. Trefilov, *Phase Transit. B* **49**, 143 (1994).
 - ⁵⁹V. I. Nizhankovski, M. I. Katsnelson, G. V. Peschanskikh, and A. V. Trefilov, *JETP Lett.* **59**, 733 (1994).
 - ⁶⁰V. S. Egorov and A. I. Fedorov, *JETP Lett.* **58**, 959 (1983).
 - ⁶¹N. V. Bashkatov and N. L. Sorokin, *Sov. Phys. Solid State* **31**, 910 (1989).
 - ⁶²V. Y. Irkhin, M. I. Katsnelson, and A. V. Trefilov, *J. Magn. Magn. Mater.* **117**, 210 (1992).